Society For Biomaterials

The effect of ethylene oxide sterilization on the surface chemistry and *in vitro* cytotoxicity of several kinds of chitosan

Rodrigo França,[1] Doris A. Mbeh,[2] Taraneh Djavanbakht Samani,[2] Canh Le Tien,[3] Mircea A. Mateescu,[3] L'Hocine Yahia,[2] Edward Sacher[2,4]

[1]Department of Restorative Dentistry, University of Manitoba, Winnipeg, Manitoba, Canada R3E 0W2
[2]Laboratoire d'Innovation et d'Analyse de Bioperformance, École Polytechnique de Montréal, Montréal, Québec, Canada H3C 3A7
[3]Département de Chimie and Centre Pharmaqam, Université du Québec à Montréal, Montréal, Québec, Canada H3C 3P8
[4]Regroupement Québecois de Matériaux de Pointe and Département de Génie Physique, École Polytechnique de Montréal, Montréal, Québec, Canada H3C 3A7

Received 16 October 2012; revised 11 February 2013; accepted 17 February 2013
Published online 7 June 2013 in Wiley Online Library (wileyonlinelibrary.com). DOI: 10.1002/jbmb.32964

Abstract: The surfaces of three chitosan samples, differing only in their degrees of deacetylation and of carboxyethyl chitosan were chemically characterized by X-ray photoelectron spectroscopy, time-of-flight secondary ion mass spectroscopy, X-ray diffraction, and Fourier transform infrared, both before and after sterilization with ethylene oxide. Unexpected elemental ratios suggest that surface chemical modification occurred during the processing of the original chitin, with further surface modification on subsequent sterilization, despite previous reports to the contrary. Cell viability was evaluated by direct contact methyl thiazole tetrazolium and lactate dehydrogenase assays between the chitosan particles and A549 human epithelial cells, which demonstrated that the modifications incurred on sterilization are reflected in biocompatibility changes. All the samples were found to be biocompatible and nontoxic before sterilization and remained so subsequently. © 2013 Wiley Periodicals, Inc. J Biomed Mater Res Part B: Appl Biomater, 101B: 1444–1455, 2013.

Key Words: biocompatibility, chemical modification, chitosan, cytotoxicological evaluation, ethylene oxide sterilization, surface characterization

How to cite this article: França R, Mbeh DA, Samani TD, Tien C, Mateescu MA, Yahia L, Sacher E. 2013. The effect of ethylene oxide sterilization on the surface chemistry and *in vitro* cytotoxicity of several kinds of chitosan. J Biomed Mater Res Part B 2013:101B:1444–1455.

INTRODUCTION

Chitosan (Ch) is a biocompatible polymer that is biodegradable, nontoxic, and self-adhesive. It is primarily composed of 2-amino-2-deoxy-β-D-glucopyranose repeat units, retaining a small amount of 2-acetamido-2-deoxy-β-D-glucopyranose residues and is the second most abundant and renewable natural polymer after cellulose. It is commonly found in the exoskeletons and cuticles of many invertebrates and in the cell walls of most fungi and some algae.[1] It is characterized either by the degree of acetylation of amino groups or by the degree of deacetylation (DD) of *N*-acetylamino groups. When the number of *N*-acetyl-D-glucosamine units is greater than 50%, the biopolymer is called chitin; when it is lower, it is called Ch (Figure 1).[1,2] Chitin and Ch are of commercial interest, due to their higher percentages of amine/amide functions, compared with synthetically substituted biopolymers,[2] making them attractive for medical use.

Ch is soluble in aqueous acids but insoluble in neutral or aqueous bases, as well as numerous other solvents, which limits its applicability. The amino group at the highly nucleophilic C2 position may be used to modify Ch, so as to obtain physicochemical or biological properties desired for specific applications. For example, Ch has been modified by glutaraldehyde cross-linking, to prepare "intelligent" drug delivery systems,[3] by carboxymethylation, to repair and regenerate bone tissue,[4] and by conjugation with sulfate, as a blood anticoagulant factor activator.[5] Recently, Tran et al.[6] treated Ch with acrylic acid to obtain carboxyethyl chitosan (CEC), which was used as a matrix for the controlled release of ibuprofen and famotidine; in contradistinction to Ch, CEC is soluble not only in acid but also in aqueous media with neutral or higher pH values, depending on its degree of carboxyethylation. This solubility, over a larger pH range, is important for various biomedical uses, including gene delivery.

Ch is also widely employed when in contact with corporeal fluids or implanted within the body, where sterilization is required. The method chosen for sterilization must be carefully selected because the physical, mechanical, and biological properties of biomaterials may be negatively affected by it.

Correspondence to: E. Sacher (e-mail: edward.sacher@polymtl.ca)
Contract grant sponsor: Natural Sciences and Engineering Research Council of Canada and NMD

© 2013 WILEY PERIODICALS, INC.

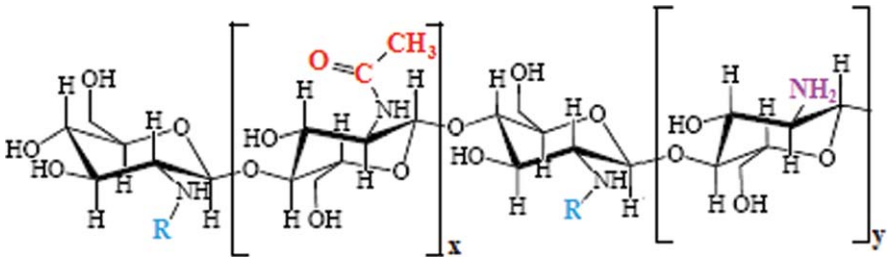

FIGURE 1. Chemical structure of chitin or chitosan. When R = $-COCH_3$ and x > 50%, chitin; when R = H and y > 50%, chitosan. [Color figure can be viewed in the online issue, which is available at wileyonlinelibrary.com.]

Several sterilization methods can be used; here, we consider the use of ethylene oxide (EtO), which was recently the subject of an extensive review.[7] Although that review concentrated on EtO sterilization, it also mentioned, and gave references to, other sterilization methods, including autoclaving, dry heat, and ultraviolet and γ-radiation.

EtO is very useful as a sterilization agent: sterilization proceeds through the direct alkylation of cellular constituents of organisms, leading to denaturation. The method has advantages such as effectiveness at low temperatures, high penetration, and compatibility with a wide range of materials. Nonetheless, EtO is flammable and explosive, it may produce toxic residues, and it reacts with functional groups, such as the amine in Ch.[7] To reduce both its toxic effects and its flammability, EtO is generally mixed with inert gases, such as fluorocarbons and CO_2. To overcome some of its drawbacks, strict rules have been established concerning its use in sterilization, such as those promoted by the American National Standard ANSI/AAMI ST27–1988.[8] Despite various studies involving the use of Ch and EtO, information about the effects of this sterilization method on the surface properties of the materials remains limited.[2]

The aim of this study is to evaluate the effects of EtO sterilization on Ch and its derivative, CEC, and to establish the relationship between the physicochemical properties of their surfaces and their *in vitro* cytotoxicity test results. In particular, our use of X-ray photoelectron spectroscopy (XPS), which probes ~5 nm of the outer layer of Ch, and time-of-flight secondary ion mass spectroscopy (TOF-SIMS), which probes its first few monolayers, is designed to aid in the comprehension of our cytotoxicity results, obtained on contacting these same outer layers.

EXPERIMENTAL

Materials

Chitosans. Four kinds of Ch were used in this study: those with DD values of 79% (Ch79), 85% (Ch85), and 95% (Ch95), as well as CEC. The three Ch samples were purchased from Marinard Biotech (Rivière-au-Renard, QC, Canada); CEC was obtained by the carboxyethylation of Ch95, as described below. Concerns over chemical modifications during reprocessing restricted us to using the samples as received. Because of this, the effects of particle size and shape were not considered here. These effects will, however, be discussed in a follow-on paper on the distribution of prodrug nanoparticles in Ch microparticles of various sizes.

Cell line and culture medium. The A549 cell line (CCL-185), obtained from ATCC, was used for the proliferation tests. It is a human Caucasian lung carcinoma type II epithelial cell and was grown in Dulbecco's modified eagle medium (DMEM), supplemented with 10% heat-inactivated fetal bovine serum (Sigma–Aldrich) and 1% penicillin/streptomycin (Gibco Laboratories), to control bacterial contamination. It was maintained at 37°C in a humidified atmosphere of 5% CO_2 and 95% air; no contamination was detected during the experiments. The culture medium used was identical to the growth medium.

Reagents. Trypsin-EDTA (Gibco/Invitrogen) was used to collect the undamaged cells. The yellow tetrazolium dye used in the methyl thiazole tetrazolium (MTT) test, 3-(4,5-dimethylthiazole-2-yl)−2,5-triphenyl tetrazolium bromide, was purchased from Trevigen; both the reagent and the detergent solution are supplied ready for use. The lactate dehydrogenase (LDH) cytotoxicity detection kit was purchased from Roche.

Methods

CEC synthesis. CEC was obtained by treatment of Ch95 (MW ~400 kDa) with acrylic acid (Sigma-Aldrich), as described by Tran et al.[6] Briefly, 10 g of Ch were dispersed in 490 mL of distilled water, and 10 mL of acrylic acid was added. After 4 h at 80°C, the final pH of the solution was adjusted to 7.0; the CEC was precipitated with added methanol, collected by filtration, washed three times with pure acetone and dried in an incubator at 40°C for 72 h. The degree of substitution was confirmed by elemental analysis (Fisons model EA-1108 Element Analyser) as ~0.45.

***Chitosan* sterilization with ethylene oxide.** All the samples, in the form of powders, were sterilized with EtO; however, only Ch95 and CEC were used for the biocompatibility tests because they, alone, were amenable to homogeneous dispersion in the culture medium. The sterilizations were performed by exposure to Honeywell Oxyfume-30 (30% EtO and 70% CO_2) for 8 h at 40°C and 40%–50% relative humidity. An initial vacuum of 400 mmHg (53.3 kPa) was applied for 15 min, and then 600 mg/L of Oxyfume-30 was

added until the chamber reached a pressure of 0.5 kgf/cm^2 (49.0 kPa). After the incubation period, a 400 mmHg vacuum was reestablished. The samples were purged with N_2 several times to remove residual EtO and stored at room temperature for at least 1 week before testing.

Chitosan characterizations. At least four replicates were used in each case. All the samples were kept in a dust-free, moisture-free atmosphere until used. With the exception of X-ray diffraction (XRD), run under ambient atmosphere, all the other techniques are run in under moisture-free conditions; because XRD is used to characterize crystalline forms, it is unaffected by the presence of moisture.

Photoacoustic Fourier transform infrared (FTIR) spectroscopy. Two hundred sixty-one FTIR scans of each powder sample were co-added on a Bio-Rad FTS 6000 spectrometer, in the range of 400–4000 cm^{-1}, using a He-purged MTEC 300 photoacoustic cell, with the spectrometer resolution set at 4 /cm.

XRD. Analyses were carried out using a PANalytic X'Pert MPD, with Cu Kα radiation ($\lambda = 1.542$ Å), generated at 50 kV, 40 mA. The 2θ range, 15°–80°, was covered in 0.02° steps, and the diffraction patterns were analyzed using the X'Pert HighScore software accompanying the instrument, with comparisons against standards from the stored JCPDS cards.

XPS. C1s, O1s, and N1s spectra of the various samples were obtained on a VG ESCALab 3 Mk II, using nonmonochromated Mg Kα radiation (1253.6 eV), at a power setting of 300 W, having an instrument resolution of 0.7 eV. When two peaks differ in energy by less than this amount (e.g., C-C and C-NH differ by ~0.3 eV), they cannot be separated with confidence; in such a case, they are subsumed into one peak. The samples were deposited onto copper sample stubs, using two-sided adhesive Cu tape. The base pressure during scanning was less than 1×10^{-9} torr. Electrons were detected at a perpendicular take-off angle, using 0.05 eV steps, and spectra were analyzed using the VG Avantage software. No Cu spectrum was visible, indicating a thick sample deposit.

TOF-SIMS. Positive and negative ion spectra, obtained with an ION-TOF IV TOF-SIMS, using a 15 kV Bi^+ primary ion source, were acquired at masses up to 500. The primary ion dose was maintained at less than 10^{12} ions/cm^2, so as to ensure static conditions. Positive ion spectra were calibrated to the H^+, H_2^+, C^+, CH^+, CH_2^+, CH_3^+, $C_2H_3^+$, $C_2H_5^+$ $C_3H_5^+$, $C_3H_7^+$, $C_4H_5^+$, $C_4H_7^+$, and $C_4H_9^+$ peaks, and negative ion spectra were calibrated to the C^-, CH^-, C_2^-, C_2H^-, C_3^-, and C_3H^- peaks before data analysis. Sample spectra were obtained over an area 50 μm × 50 μm, rastered in random mode, 128 by 128 pixels, with an emission current of 1.0 μA in bunch mode.

Scanning electron microscopy (SEM). Photomicrographs were obtained with a JEOL JSM-7600TFE microscope. Samples were deposited onto an amorphous carbon ribbon and, subsequent to the deposition of a layer of amorphous carbon, inserted into the instrument. Images were obtained at a 2 keV accelerating voltage.

Relative dispersibilities of the various types of chitosan in the culture medium. It was initially intended to analyze the biocompatibilities of all the sample dispersions (Ch79, Ch85, Ch95, and CEC) in direct contact with cells, for the purpose of obtaining light microscopy images. However, as mentioned earlier, only the latter two were homogeneously dispersible in the culture medium; they were added to the medium, at a concentration of 1 mg/mL, with 2 mL of the cell suspension, and were analyzed by light microscopy at 20× magnification. This concentration was used only for obtaining light microscopy images, with various other concentrations used for Ch preparation, as described below.

Biological assays.

Cytotoxicity. These studies were performed by direct contact of Ch particles with A549 cells. One hundred microliters per well of cell suspension (1.0×10^5 cells/mL) in culture medium were inoculated in the 96-well microplate and permitted to grow for 24 h, at 37°C, in a humidified atmosphere of 5% CO_2 and 95% air. The samples, both before and after sterilization, were suspended in DMEM at several concentrations (25, 50, 75, and 100 μg/mL), a range often used in the literature,[9,10] with 0 μg/mL as control at room temperature. After 24 h, the medium in the microplate containing cells was removed and replaced with the one containing different concentrations of Ch particle suspensions (0–100 μg/mL) for another 24 h. Cell viability was determined by both MTT and LDH tests.

MTT. Mitochondria play a critical role in cellular function through aerobic adenosine triphosphate production.[11] The MTT assay uses the yellow tetrazolium salt, 3-(4,5-dimethylthiazole-2-yl)−2,5-diphenyl-tetrazolium bromide, to measure cell viability through tetrazolium compound bioreduction by viable cells to give a colored formazan product. The conversion in the viable cells is done by nicotinamide adenine dinucleotide phosphate or nicotinamide adenine dinucleotide, catalyzed by dehydrogenase enzymes. The formazan absorbance is measured at 570 nm and is related to the number of viable cells.[12] Following the manufacturer's directions,[10] the exposure media containing the Ch solutions were aspirated (cells still adhered to the well bottom), and each well was rinsed with 200 μL of 1% phosphate-buffered saline (Invitrogen, 10x Gibco Phosphate-Buffered Saline, pH 7.2). One hundred microliters of medium were then added to each well, along with 10 μL of MTT reagent. After incubation for 4 h at 37°C, under 5% CO_2, 100 μL of Invitrogen detergent was added to each well to insure solubilization of the formazan crystals. The plate was held in the dark, at room temperature, and read after 3 h. The optical density values were determined at 570 nm, using a Beckman microplate reader. The relative cell viability (%) results were computed by dividing the absorbance values from wells

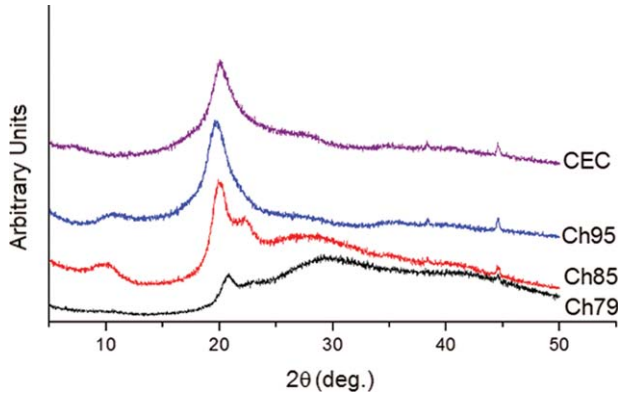

FIGURE 2. XRD spectra of chitosan samples before sterilization. [Color figure can be viewed in the online issue, which is available at wileyonlinelibrary.com.]

with sampled cells by those from the control wells (i.e., wells with only cells and no Ch), as follows:

$$\text{Cell viability}\,(\%) = (\text{Sample absorbance} / \text{Control absorbance}) \times 100.$$

LDH assay. LDH, a stable enzyme present in the cytosol, is released upon cell lysis. This assay permits the determination of compounds that induce alterations in cell integrity. It is based on the measurement of LDH released from the cytosol of dead or plasma membrane-damaged cells and was performed on the culture supernatant from the plates used for the MTT assay. After the incubation of cells with the different types of Ch, the supernatants (100 μL) were transferred to a 96-well plate for LDH assay, and the cells that remained in the plates were used for the MTT assay. Equal volumes of the reaction mixture were added to each well. Absorbance was measured at 492 nm, and the cytotoxicity, in percent, was calculated relative to Triton X-100 as the positive control (100% cytotoxicity) and the cells in the culture medium as the negative control (0% cytotoxicity) as follows:

$$\text{Cytotoxicity}\,(\%) = ((S-C)/(T-C)) \times 100,$$

where S is the measured value, C is the negative control value, and T is the positive control value.

RESULTS

Morphological characterization

XRD. As noted earlier, Ch can present different crystalline patterns. Native chitin has three anhydrous crystalline polymorphs, α, β, and χ, depending on its source.[13,14] The α−chitin, from which our samples are derived, the most abundant of the three polymorphs, has a tightly compacted orthorhombic cell, formed by alternating sheets of parallel and antiparallel chains. The β-chitin adopts the parallel form with a monoclinic unit cell, and the χ-chitin structure has not been completely identified.[14] The XRD patterns of all our samples, before sterilization (Figure 2), present a peak at $2\theta = 20^\circ$, and the degree of crystallinity increases with the DD value. This difference in crystallinity may reflect the fact that Ch chains with higher degrees of deacetylation are more compact, with a greater number of amine groups facilitating hydrogen bonding[15] and crystal formation. An additional peak appears at $2\theta = 10^\circ$, possibly indicating another crystal form. This structural parameter influences both physicochemical[16] and biological properties.[17] The XRD patterns do not change on sterilization. This is because, as shown below, EtO affects only the outer surface of the sample.

SEM. The photomicrographs in Figure 3 are purposely presented at slightly different magnifications, to advantageously demonstrate the structures we discuss; they show the morphological structures of Ch79 [Figure 3(A)], Ch85 (3B), and Ch95 (3C), with orderly, arranged layers forming fibrils. In contradistinction, for CEC (3D), the particles were replaced by a rougher, irregular shape that indicates an alteration of the Ch structure on carboxyethylation.

Surface chemical characterization

FTIR. Spectra, found in Figure 4, compare Ch95 and CEC, with those of the sterilized materials in the inset. The principal vibrational band positions and their group attributions[18] are presented in Table I. Because bands from different chemical structures fall at similar positions, little attributable difference is found among the spectra. For example, all the samples display strong vibrations at 1645 and 1584 cm^{-1}, which have, in the past, been attributed to amide I and II vibrations. However, because only 20% or less of the nitrogen in our samples occurs as amide, the remaining nitrogen being amine, these attributions are unlikely to be unique. Because amine deformation vibrations also produce strong bands in the 1640–1575 cm^{-1} region,[19] it is likely that they, too, contribute to these peaks.

The inset to Figure 4 indicates that there are no strong differences among samples before and after EtO sterilization. This is surely because any new vibrational peaks are limited to several nm of sample surface, while FTIR probes 2–3 μm in depth.

XPS. Survey spectra, found in Figure 5, present the elemental compositions, at a probe depth of ∼5 nm for C, N, and O (attenuation lengths are $\sim 1.5 \pm 0.2$ nm for all these elements, with the probe depth being 3× the attenuation length); they are given in relative percentages, before and after sterilization. The CEC surfaces were also found to contain trace concentrations of Na and Cl, retained from the fabrication process. The data show an expected decrease in the percentage of C on increasing DD from Ch79–Ch95, but not for CEC. The percentage of nitrogen atoms expected for CEC should be about the same as in Ch95, but the XPS results show that it suffers a slight, but noticeable, diminution after carboxyethylation: this is because an increase of C and O leads to an apparent relative decrease of N.

Referring to the chemical structure of Ch, in Figure 1, Table II lists the binding energies of the high resolution XPS peaks for the chemical groups that are expected. Table III

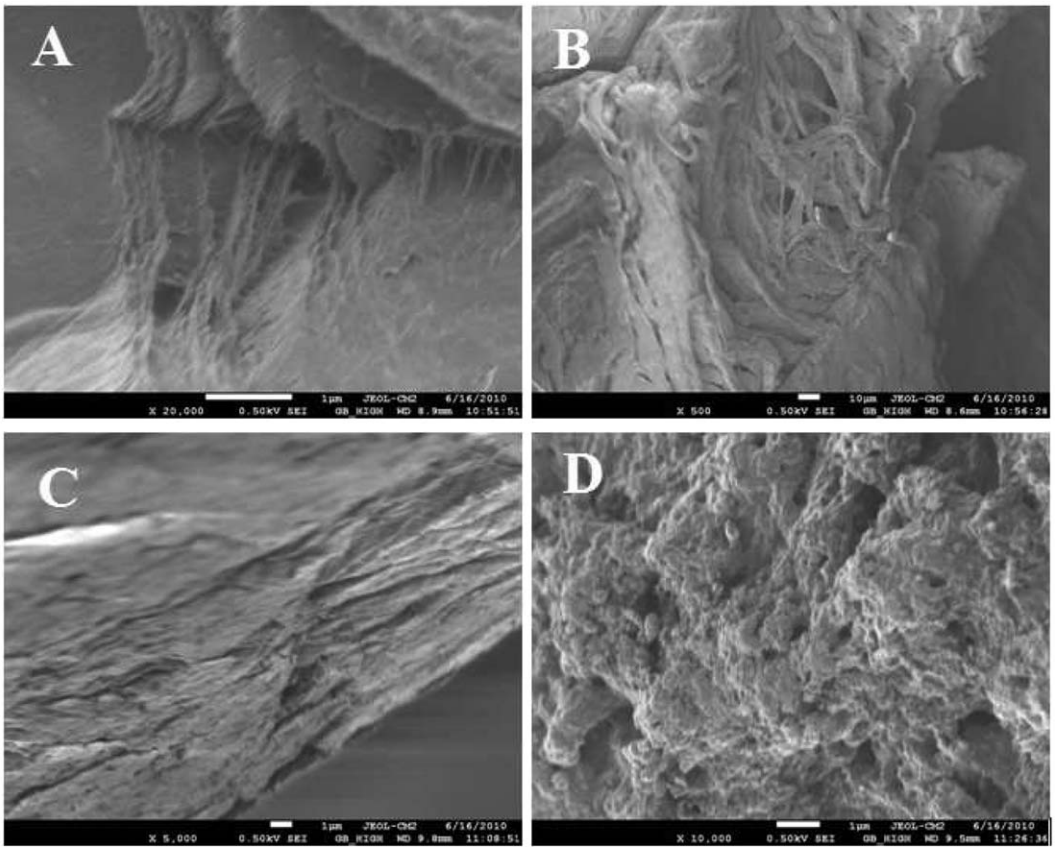

FIGURE 3. SEM photomicrographs of (A) Ch79, (B) Ch85, (C) Ch95, and (D) CEC, before sterilization.

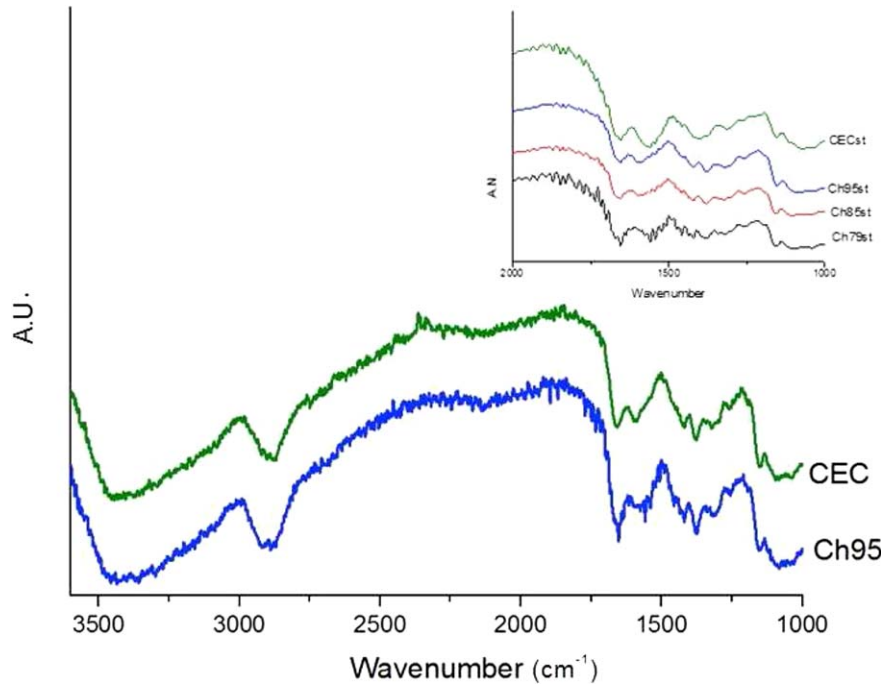

FIGURE 4. FTIR spectra of chitosan samples before and after sterilization (st) with ethylene oxide. [Color figure can be viewed in the online issue, which is available at wileyonlinelibrary.com.]

TABLE I. Infrared Bands Found and Their Attributions

Band (cm^{-1})	Attribution
3450–3290	O-H stretching
3500–3400	N-H_n stretching
2890–2860	C-H_n stretching
1690–1645	C=O stretching
1600–1580	N-H bending
1560–1415	Symmetric and asymmetric O-C=O stretching
1410–1420	CH_2 bending
1380–1370	CH_3 symmetric deformation
1160–1150	C-O-C asymmetric stretching, C-N stretching
1020–1030	C-O skeletal stretching
1000–800	C-H deformation

and Figure 6 show that the surfaces of all the samples have chemical compositions that differ from those that are expected. For example, Ch79 has five C1s peaks (recall that C-C and C-N are subsumed into one peak), and the atomic percentages, both before and after contact with EtO, are found to be different than those expected. All samples manifest two or more O1s peaks, at positions that imply the presence of -COOH. CEC has two N1s peaks, quite different from what is expected, because both amine and amide appear at essentially the same position. Unmistakably, at least at the sample surfaces, the structures found do not resemble that in Figure 1.

Table II displays the component peak positions expected from high-resolution XPS. The C1s spectra of Ch79, Ch85, and Ch95 were predicted to have three peaks: the first peak at 285.0 eV is attributed to aliphatic carbon from C-C and C-N groups, and any adventitious carbon; the second peak at 286.4 eV is attributed to alcohol (C-OH) and ether (C-O-C) groups; the third peak at 288.0 eV is attributed to O-C-O and amide carbonyl. However, Ch79, Ch79st, and Ch85st show an unexpected fourth peak, at ~289.0 eV, which is attributed to -COOH; CEC and CECst also have these four peaks. In addition, both Ch79 and Ch79st have another, unidentified, peak at >291 eV, indicating an unidentified C with a high positive charge.

For the O1s spectrum, only one peak, at ~533.5 eV, is expected for Ch79, Ch85, and Ch95, because the ether and alcohol groups have very similar binding energies. In fact, two or more peaks are found for all the samples, which indicates the presence of other oxidized C species, confirming what was found in the C1s spectrum.

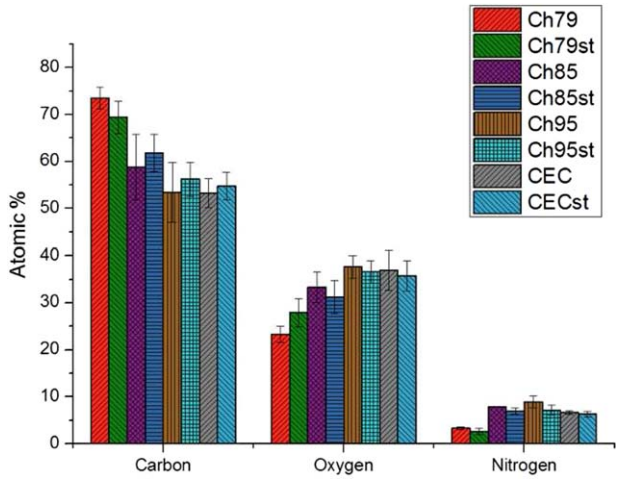

FIGURE 5. XPS-determined relative surface compositions before and after sterelization (st) with ethylene oxide. [Color figure can be viewed in the online issue, which is available at wileyonlinelibrary.com.]

For the N1s spectrum, one peak, at ~399.0 eV, is expected, because N, in both amines and amides, appears at the same binding energy. The Ch79 samples show only one peak, at ~401.2 eV, 2 eV higher than for an amine (~399 eV), possibly indicating the presence of an ammonium salt ($R\text{-}NH_3^+$) or, more probably, an amine oxidation product (e.g., nitroso); oxidized amine was also found in our recent study of the preparation of magnetite–silica–amine-terminated silane core-shell-shell nanoparticles.[20] CEC, even before sterilization, has two peaks, at ~398.9 and 400 eV, the latter suggesting slight amine oxidation (e.g., hydroxylamine or oxime).

While both Ch79 and Ch79st manifest unexpectedly high binding energy C1s and O1s components, this is due to neither referencing nor charging problems. Not only are the N1s components properly energy corrected but also the same spectra were obtained for each replicate. The reason for the presence of these peaks is currently unknown.

To summarize the XPS results before sterilization, all the samples, irrespective of their DD, exhibit additional C1s, O1s, and N1s peaks, indicating a modification of the expected surface chemistry. This has been commonly found in the literature. Indeed, without exception, recent publications,[21–23] using Ch samples of DD values similar to this study, have deemed it necessary to use 3–4 C1s peaks, 2–3

TABLE II. Expected XPS Peaks, Attributions, and Ratios

	FWHM[a] (eV)	Peak Attribution		BE (eV)	Peak Ratios[b] 79	85	95	CEC
Carbon	1.7	*C1s A*	CH-CH,C-NH	285.0	2	2	2	2
		C1s B	C-OH, C-O-C	286.4	5	5	5	5
		C1s C	-N-C=O	288.0	0.21	0.15	0.05	0.05
Oxygen	1.8	*O1s A*	C=O	532.7				1
		O1s B	C-O-C, C-OH	533.3				2
Nitrogen	1.7	*N1s*	C-NH, N-CO	399.7				

[a] Values used in our laboratory peak separations.
[b] Values based on the reported amount of amide.

TABLE III. XPS Peaks Found

	C1s					N1s		O1s			
	A	B	C	D	E	A	B	A	B	C	D
Ch79	285	286.8	288.5	290.1	291.9	401.2		533.2	536	537	
Ch79st	285	286.7	288.4	289.9	291.5	401.9	403.2	532.6	534.8	536.3	537.5
Ch85	285	286.4	287.8			399.2		531.9	532.9		
Ch85st	285	286.4	288.1			399	399.8	531.4	532.7		
Ch95	285	286.5	288.1			399.3		531.4	532.8		
Ch95st	285	286.2	287.6			399.2	400	531.6	532.9		
CEC	285	286	286.9	288.3		398.9	400	530.8	532.2	533.2	
CECst	285	286.3	287.5	288.9		399.9	400.8	531.6	532.9	533.9	

O1s peaks, and 2–3 N1s peaks to fit their XPS results. The extra peaks are variously described as coming from contaminants and amine salts. Relative atomic percentages of our samples are found in Figure 7.

The EtO sterilization process is clearly chemical, in nature: EtO is a powerful direct alkylating agent. The addition of alkyl groups to microorganisms, which bind to their hydroxyl, amino, and carboxylic acid groups, limits normal cellular metabolism and the ability to reproduce.[3] Our XPS analysis has confirmed that EtO reacts with the sample surfaces, resulting in the appearance of new species. We find that, in addition to the (principal) alkylation reactions, which adds hydroxyethyl ($-CH_2-CH_2-OH$) moieties to hydroxyl, amino and carboxylic acid groups, the particle surface appears to have undergone a (minor) oxidation, particularly noticeable in the N1s spectra: as indicated earlier, the N1s spectra of the Ch and CEC samples all display an additional higher energy peak on EtO sterilization, which can be attributed to amine oxidation; this is confirmed by their IR spectra.[18] The O1s spectrum of Ch79st manifests a new peak, at 534.8 eV, not present in Ch79, indicating the oxidation of a previously existing group.

To summarize the overall XPS results, the Ch sample surfaces appear to have suffered chemical modifications both on processing from chitin and EtO sterilization. This has prompted us to avoid further chemical modifications that would result from reprocessing the as-received samples so as to vary size and shape.

TOF-SIMS. Only Ch95 and CEC were analyzed by TOF-SIMS. Figure 8(a,b) shows the positive and negative spectra of the unsterilized Ch95, and Figure 8(c,d) shows those of the sterilized Ch95. Figure 8(e,f) shows the positive and negative spectra of the unsterilized CEC, and Figure 8(g,h) shows those of the sterilized CEC. Adventitious hydrocarbon fragments were observed in all TOF-SIMS spectra, indicating surface deposition from the atmosphere during manufacture. Na and Cl impurities were observed for both Ch95 and CEC.

Following sterilization, no additional peaks, which might be attributable to sterilization, were observed, but relative intensities of both positive and negative mode peaks were decreased, probably due to EtO-induced surface modifications. The CNO^- fragment (42 D) was clearly observed in the logarithmic intensity spectra (data not shown) of all the samples, in support of the XPS data cited above, indicating the presence of amide (N-C=O) and/or amine oxidation (C-N=O). On sterilization, the observed CNO^-:CN^- ratios (m = 42:26) increased 20% for Ch95 and 33% for CEC, which can be only due to amine oxidation; for four independent determinations, these increases were constant to within 1% for Ch95 and 4% for CEC. This indicates that the increase in the CNO^-:CN^- ratios was due to amine oxidation during sterilization and also helps to explain why TOF-SIMS found no new peaks on sterilization.

Biological Assays

Relative dispersibilities of Ch95 and CEC in the culture medium. To compare the dispersion properties of the samples, they were suspended in culture medium, at a concentration of 1 mg/mL,[24,25] and analyzed, by light microscopy, at 20× magnification. Figure 9 compares Ch95 (9A) and CEC (9B): a higher dispersibility was found for CEC, probably due to the presence of polar carboxylic acid groups.

***Direct contact MTT* cell viability assay.** MTT cell viability was assessed following a 24 h exposure of the cells to Ch 95 and CEC. The reader is reminded that cell viability values are given as percentages of the negative control.

Ch95 showed little or no increase in cell growth viability as a function of concentration (Figure 10), either before or after sterilization. However, the viability increased subsequent to sterilization. For CEC, the viability decreased with concentration both before and after sterilization, although that following sterilization was greater. For CECst, a maximum in viability occurs at a concentration below 25 μg/mL, the lowest concentration explored in this study.

These direct contact cytotoxicity assays show that all the sterilized samples are biocompatible, the cellular viability being 80% or greater, when compared with the control. Ch95 appears to undergo a slight increase in cell viability with concentration, near 100% cell viability. For Ch95st, there is a marked increase in viability, above 110% of the control; such a response indicates the stimulation of A549 cellular proliferation as a result of sterilization.

By comparison, CEC presents good cell viability, with slight decreases at higher concentrations. As with Ch95, sterilization increases cell viability by about 15%–20%, with the maximum cell viability lying at or below the lowest concentration used (25 μg/mL). Clearly, the surface modification incurred by sterilization has a similar effect for both materials.

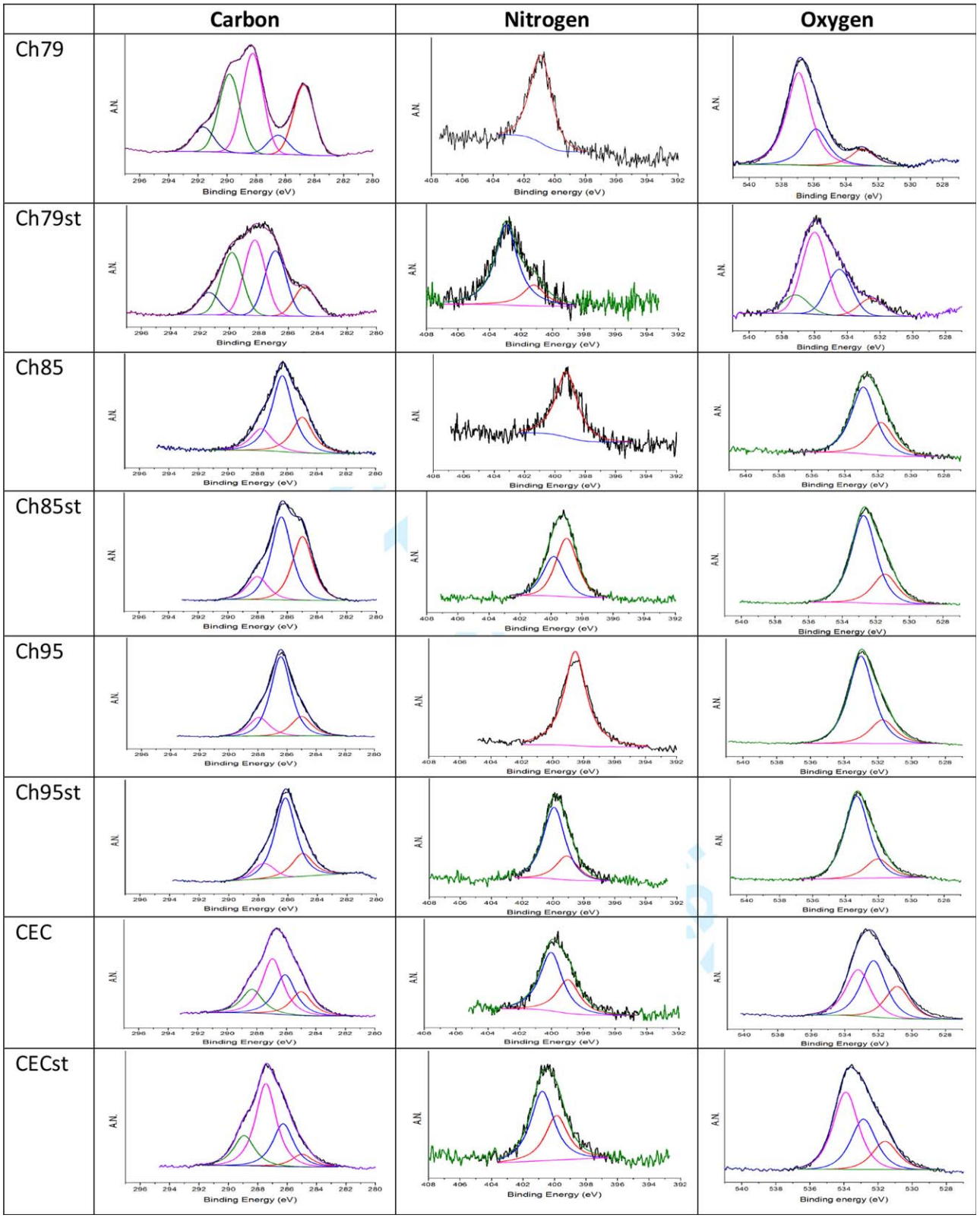

FIGURE 6. High-resolution XPS component spectra before and after sterilization (st) with ethylene oxide. [Color figure can be viewed in the online issue, which is available at wileyonlinelibrary.com.]

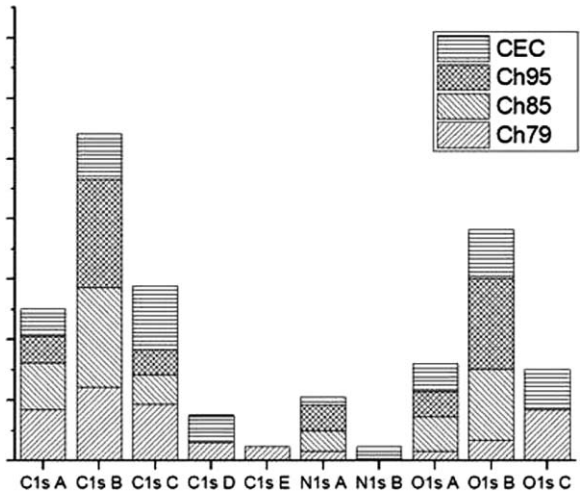

FIGURE 7. Relative atomic percentages of XPS-determined C1s, N1s and O1s peak components of the chitosan samples before sterilization.

LDH assay. LDH, a stable enzyme present in the cytosol, is released upon cell lysis. This assay permits the investigation of compounds that induce alterations in cell integrity; it was performed to measure the membrane-damaging effects of Ch95 and CEC at different concentrations via the quantity of LDH in the culture media. Based on the MTT assay, the different types of Ch were practically nontoxic after 24 h of incubation. To elucidate any membrane-damaging effect caused by these samples, their influence on LDH release was investigated using Triton-X as a positive control, as shown in Figure 11. The effect of Ch particles on the membrane integrity of the A549 cell line was found to be negligible and independent of both the type of Ch and the concentration used. No bacterial contamination was detected, on 24 h of cell incubation, for any of the samples.

DISCUSSION

Our initial interest in Ch included the facts that it possesses a highly reactive amine group and that it is biocompatible.

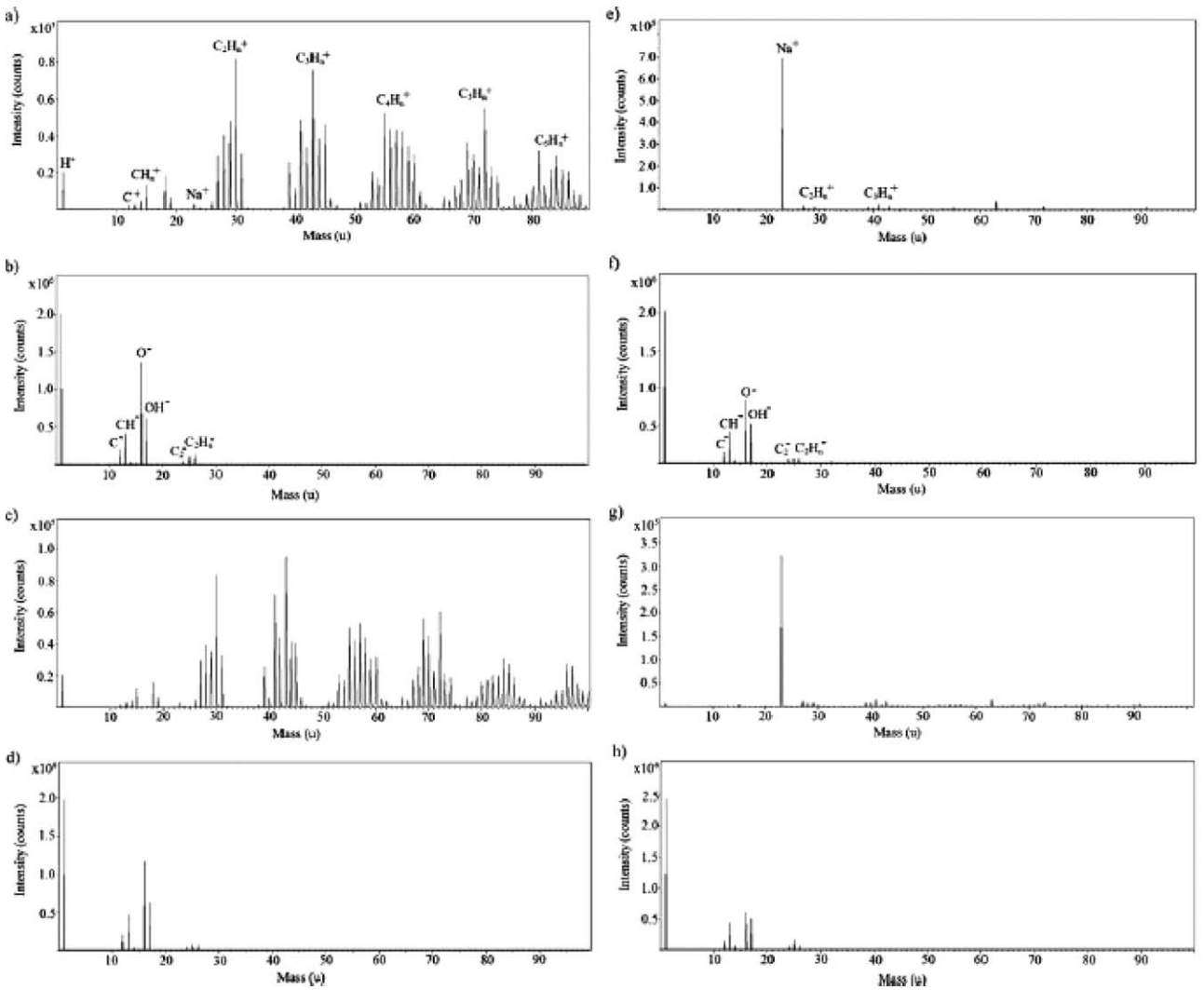

FIGURE 8. TOF-SIMS positive (A) and negative (B) spectra of unsterilized Ch95; positive (C) and negative (D) spectra of sterilized Ch95; positive (E) and negative (F) spectra of unsterilized CEC; and positive (G) and negative (H) spectra of sterilized CEC.

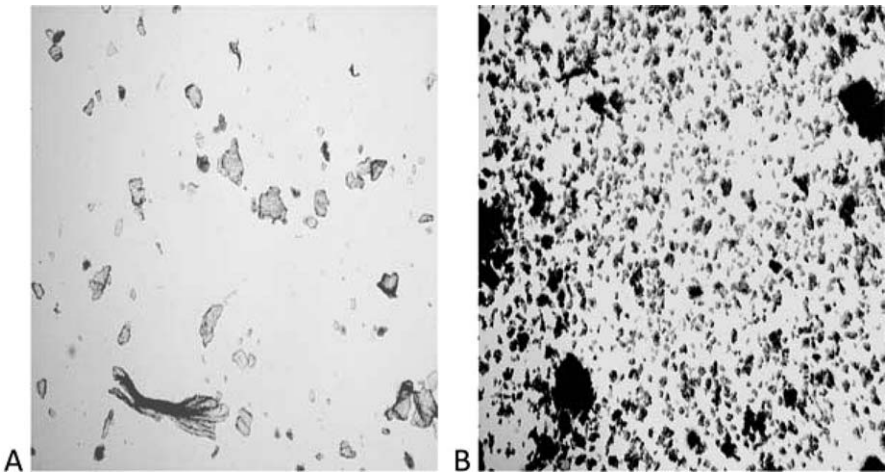

FIGURE 9. Chitosan samples suspended in F-12K; (A) Ch95 and (B) CEC. All particle suspensions were at a concentration of 1 mg/mL. Magnification 20×.

It was our wish to determine how these highly desirable properties were influenced by exposure to EtO, what is probably the most common sterilization procedure used in a hospital setting. The present results reveal that chemical changes occur at the Ch surface, which may influence the ultimate use of Ch in the human body. To make these results more understandable, we have chosen to present them in the following format: we first consider what our results tell us about the chemistry of the Ch surface, because that is what will contact the body fluids on initial exposure; we next consider what our surface-sensitive techniques tell us about the changes incurred on EtO exposure; finally, we invoke our biological assays to determine whether and to what extent this exposure to EtO influences cytotoxicity.

Chitosan surface structure

The structures at the Ch surfaces are not those expected. Figure 1 represents the conventional structure of Ch. Based on that structure, Ch repeat units have six-eight C atoms (depending on the DD), three-four O atoms, and one N atom. As mentioned earlier (Table II), high-resolution XPS predicts three C components, and one each for O and N. However, all the Ch samples show two O components before sterilization. Because ether and alcohol groups have similar binding energies, the second component indicates the presence of another O-containing surface structure.

The atomic ratios of the various peaks, determined by XPS, may be used to confirm correspondence with the structure in Figure 1. For the hypothetical Ch structure, with 100% DD, the ratio expected among the C1s A, B, and C peaks is 1:5:0. Nonetheless, Figure 7 shows that the atomic ratios measured do not correspond to these ratios for any of the Ch samples. For example, Ch85 and Ch95 have the correct number of C1s peaks expected, at the correct binding energies. However, their ratios are not the expected 1:5:0.15 (where 0.15 indicates the expected acetyl contribution) for Ch85 and 1:5:0.05 for Ch95; rather, they are the substantially different values of 2.6:5:1.4 and 1.2:5:1.2, respectively. Although C1s peak A (285.0) may contain

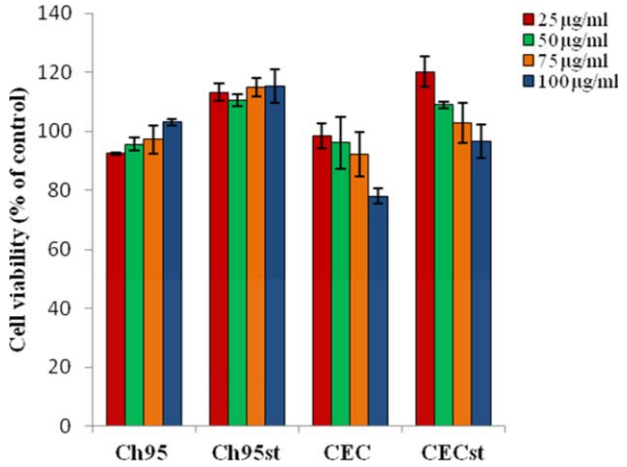

FIGURE 10. Effects of chitosan particle concentrations on A549 cell viability (direct contact). [Color figure can be viewed in the online issue, which is available at wileyonlinelibrary.com.]

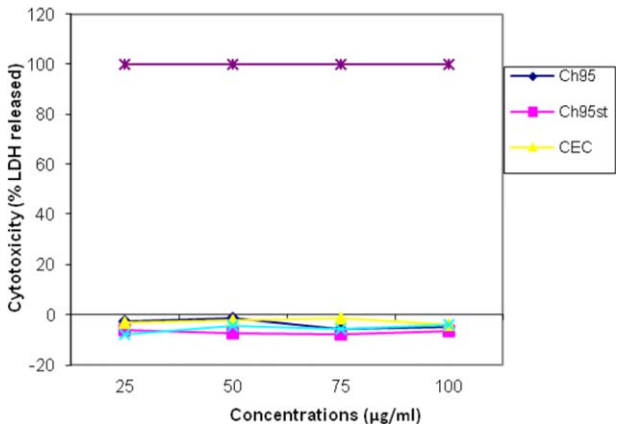

FIGURE 11. LDH assay of chitosan particles at different concentrations in A549 cell line. [Color figure can be viewed in the online issue, which is available at wileyonlinelibrary.com.]

adventitious carbon from atmosphere contamination, the ratio between C1s peaks B (286.4 eV) and C (288.0 eV) is expected to remain constant. Thus, the percentage of C-O-C and C-OH on the Ch95 surface is expected to be 100× greater than that of N-C=O, rather than the experimentally determined 4×. The reason for these unexpected ratios may be, as suggested earlier, a surface chemically modified by the processing of the original chitin, which consists of its basic deacetylation. On the other hand, it is difficult to imagine how the deacetylation process can cause the changes seen in the O1s and N1s XPS spectra, cited earlier; this must raise a question as to the extent to which the idealized structure in Figure 1 exists in the naturally occurring Ch.

EtO sterilization

Previous studies,[3,26,27] which did not use surface-sensitive techniques, found that EtO sterilization did not appear to cause polymer degradation, or changes in the physical or mechanical properties of Ch. In contradistinction, our XPS results show that on EtO sterilization, all the Ch samples, irrespective of DD, suffered surface chemical alterations (Figure 7). Specifically, the amine groups (the most reactive) underwent oxidation: Ch85 and Ch95 underwent 40% and 66% oxidation, respectively. Because the changes were not detected by FTIR, with a probe depth of 2–3 μm in the IR frequency range, the phenomenon is certainly restricted to the surface.

As the XPS data on all our unsterilized Ch samples show, the structures expected differ from those found, probably due to the processing that the raw chitin had undergone. Although it is clear that further structural changes have occurred, at all the Ch surfaces, on EtO sterilization, the present uncertainty concerning initial structures makes it difficult to specify what these changes are.

In contrast, the percentage of NH_n in CEC did not change on sterilization. This could be due to several factors: (a) the resistance of carboxyethyl amine groups (-NH-CH_2-CH_2-COOH) to attack by EtO; (b) the low reactivity of carboxylate groups with EtO; and (c) the reduced availability of free amine groups, because those available to reaction (∼45%) had already been converted to carboxyethyl amine. As mentioned earlier, the amine group is attractive for biomedical applications; the reduction of the number of such sites on the Ch surface, on EtO sterilization, reduces this attractiveness. Undeniably, because the probe depth for N is ∼5 nm in depth, our present results cannot indicate whether any of the amino groups detected are exposed for further reaction, or lying below the outer surface but still detectable, as in the case of CEC. However, our XPS results (Figure 6) clearly show that, in every case, other significant changes were noted on EtO sterilization.

These findings are supported by the TOF-SIMS results, which show decreases in relative peak intensities on sterilization, as well as increases in the CNO^-:CN^- ratios. Because this technique probes the outer few Ångströms, as opposed to nanometers (XPS) and microns (FTIR), changes seen by TOF-SIMS would be difficult to be observed by the latter two techniques and should not be overemphasized.

Cytotoxicity

The MTT cytotoxicological results on our Ch samples changed noticeably on sterilization, certainly due to the changes in surface chemistry. Recall that, due to the different dispersibilities of our Ch samples, only Ch95 and CEC could be placed in direct contact with A549 cultures to assess their cytotoxicities. The direct contact technique is considered to be a more sensitive and reliable method of determining the cytotoxicities of biomaterials, compared with the indirect contact method,[28] capable of assessing the possible toxic effects of Ch surfaces in direct contact with epithelial cells. As noted earlier, we limited this study to as-received samples, because we wished to separate out any effects due to chemical changes on reprocessing our samples into microparticles; such changes will be discussed in a follow-on paper on prodrug nanoparticles distributed in Ch microparticles.

The surface modifications detected by XPS have a real effect on the cytotoxicities of these samples. As seen in Figure 10, the sterilized samples have increased cell viabilities, although their behaviors as a function of concentration are similar to those of the unsterilized samples. This is in agreement with the previous results of Marreco et al.[8] on Ch and has been recently confirmed.[29] Clearly, the oxygenated chemical groups introduced on sterilization, whose structures need further elucidation, cause the increased viability. Despite this difference between the sterilized and the nonsterilized samples manifested in the MTT assay, the effect of Ch particles on the membrane integrity of the A549 cell line was found to be negligible, both before and after EtO sterilization, as seen in Figure 11. Additional tests may confirm the long-term enhanced proliferation presented by sterilized Ch.

We have not considered here any effects due to particle size or shape, which may play a part in Ch cytotoxicity. Neither have we measured the effect of sample solubility: CEC is known to be more soluble than Ch95, which may influence the direct contact results. These are presently being considered and will be reported on in a future article. Our results are currently limited to the confirmation that, under the constant sample dimensions considered here, Ch and CEC are biocompatible and nontoxic.[8,29–31]

CONCLUSIONS

Four Ch samples were chemically and morphologically characterized, before and after EtO sterilization. Although the FTIR and XRD results, which probe the sample volume, are in general agreement with those found in the literature, the XPS analysis, which probes the outer layers, indicates structural alterations detected at the sample surfaces both before and after sterilization. This is supported by TOF-SIMS, which shows an increase in amine oxidation on sterilization.

The retention of bulk characteristics on EtO sterilization, as indicated by XRD and FTIR, shows that the bulk is not affected. However, the surface modifications found have

clear biological ramifications. Biocompatibility assays reveal that, for unsterilized material, the effect of concentration on viability is slight, increasing for Ch95 and decreasing for CEC, but is high in both cases. EtO sterilization improves cell viability for both Ch95 and CEC, suggesting that cell proliferation has a preference for oxidized surfaces. The mechanisms involved are currently being explored in a separate study.

REFERENCES

1. Khor E, Lim LY. Implantable applications of chitin and chitosan. Biomaterials 2003;24:2339–2349.
2. Majeti NV, Ravi K. A review of chitin and chitosan applications. React Funct Polym 2000;46:1–27.
3. Thacharodi D, Rao KP. Propranolol hydrochloride release behaviour of crosslinked chitosan membranes. J Chem Technol Biotechnol 1993;58:177–181.
4. Tokura S, Tamura H. O-Carboxymethyl-chitin concentration in granulocytes during bone repair. Biomacromol 2001;2:417–421.
5. Hirano S, Tanaka Y, Hasegawa M, Tobetto K, Nishioka A. Effect of sulfated derivatives of chitosan on some blood coagulant factors. Carbohydr Res 1985;29:205–215.
6. Tran TH, Le Tien C, Gosselin P, Mateescu M-A. Carboxylated chitosan under protonated form for drug controlled release. Proceedings of the 35th Annual Meeting and Exposition of the Controlled Release Society, July 12–16, 2008, New York, USA.
7. Mendes GCC, Brandão TRS, Silva CLM. Ethylene oxide sterilization of medical devices: A review. Am J Infect Control 2007;35: 574–581.
8. Marreco PR, Moreira PL, Genari SC, Moraes AM. Effects of different sterilization methods on the morphology, mechanical properties, and cytotoxicity of chitosan membranes used as wound dressings. J Biomed Mater Res Part B 2004;71:268–277.
9. Qi L-F, Xu Z-R, Li Y, Jiang X, Han X-Y. In vitro effects of chitosan nanoparticles on proliferation of human gastric carcinoma cell line MGC803 cells. World J Gastroenterol 2005;11:5136–5141.
10. Jiang H-L, Lim H-T, Kim Y-K, Arote R, Shin J-Y, Kwon J-T, Kim J-E, Kim J-H, Kim D, Chae C, Nah J-W, Choi Y-J, Cho C-S, Cho M-H. Chitosan-graft-spermine as a gene carrier in vitro and in vivo. Eur J Pharmaceut Biopharmaceut 2011;77:36–42.
11. Hussain SM, Frazier JM. Cellular toxicity of hydrazine in primary rat hepatocytes. Toxicol Sci 2002;69:424–432.
12. Mosmann T. Rapid colorimetric assay for cellular growth and survival: Application to proliferation and cytotoxicity assays. J Immunol Meth 1983;65:55–63.
13. Souza BWS, Cerqueira MA, Martins JT, Casariego A, Teixeira JA, Vicente AA. Influence of electric fields on the structure of chitosan edible coatings. Food Hydrocoll 2010;4:330–335.
14. Minke R, Blackwell J. The structure of α-chitin. J Mol Biol 1978;120:167–181.
15. Ziani K, Oses J, Coma V, Mate JI. Effect of the presence of glycerol and Tween 20 on the chemical and physical properties of films based on chitosan with different degree of deacetylation. Food Sci Technol 2008;41:2159–2165.
16. Chatelet C, Damou O, Domard A. Influence of the degree of acetylation on some biological properties of chitosan films. Biomater 2001;22:261–268.
17. Varum KM, Myhr MM, Hjerde RJ, Smidsrod O. *In-vitro* degradation rates of partially N-acetylated chitosan in human serum. Carbohydr Res 1997;299:99–101.
18. Bellamy LJ. The Infra-red Spectra of Complex Molecules, 2nd ed. London: Methuen & Co Ltd; 1958. p 425.
19. Lawrie G, Keen I, Drew B, Chandler-Temple A, Rintoul L, Fredericks P, Grøndahl L. Interactions between alginate and chitosan biopolymers characterized using FTIR and XPS. Biomacromol 2007;8:2533–2541.
20. França R, Zhang X, Veres T, Yahia L, Sacher E. Core-shell nanoparticles as prodrugs: Possible cytotoxicological and biomedical impacts of batch-to-batch inconsistencies. J Coll Interface Sci 2013;389:292–297.
21. Amaral IF, Granja PL, Barbosa MA. Chemical modification of chitosan by phosphorylation: An XPS, FT-IR and SEM study. J Biomater Sci Polym Ed 2005;16:1575–1593.
22. Janciauskaite U, Rakutyte V, Miskinis J, Maskuska R. Synthesis and properties of chitosan-*N*-dextran graft copolymers. React Funct Polym 2007;68:787–796.
23. Ieva E, Trapani A, Cioffi N, Ditaranto N, Monopoli A, Sabbatini L. Analytical characterization of chitosan nanoparticles for peptide drug delivery applications. Anal Bioanal Chem 2009;393:207–215.
24. Wenshui X, Ping L, Jiali Z, Jie C. Biological activities of chitosan and chitooligosaccharides. Food Hydrocoll 2011;25:170–179.
25. Aiba S. Studies on chitosan: 4. Lysozymic hydrolysis of partially N-acetylated chitosans. Int J Biol Macromol 1992;14:225–228.
26. Angerer J, Bader M, Kramer A. Ambient and biochemical effect monitoring of workers exposed to ethylene oxide. Int Arch Occup Environ Health 1998;71:14–18.
27. Baier RE, Meyer AE, Akers CK, Netielle JR, Maanaghan M, Carter JM. Degradative effects of conventional steam sterilization on biomaterial surfaces. Biomater 1982;3:241–245.
28. Saw TY, Cao T, Yap AUJ, Ng MML. Tooth slice organ culture and established cell line culture models for cytotoxicity assessment of dental materials. Toxicol In Vitro 2005;19:145–154.
29. Yang Y-M, Zhao Y-H, Liu XH, Ding, F, Gu XS. The effect of different sterilization procedures on chitosan dried powders. J Appl Polym Sci 2007;104:1968–1972.
30. Mi FL, Tan YC, Liang HF, Sung HW. *In-vivo* biocompatibility and degradability of a novel injectable-chitosan-based implant. Biomater 2002;23:181–191.
31. San Juan A, Montenbault A, Gillet D, Say JP, Rouif S, Bonet T, Royaud I, David L. Degradation of chitosan-based materials after different sterilization treatments. IOP Conf Ser Mater Sci Eng 2012;31:012007.